

Influence of surface roughness on the flow behavior in TVF and WVF

L. Pokorny¹, N.J. Saikia¹, Y. Takeda¹ and E.J. Windhab¹

¹Laboratory of Food Process Engineering, Institute of Food, Nutrition and Health
ETH Zurich, Schmelzbergstrasse 9, 8092 Zurich, Switzerland

Taylor Couette flow starts with a laminar azimuthal state, over going into an intermediate state with Taylor vortices by increasing rotational speed. These vortices are characterized by their axisymmetric toroidal shape. When exceeding a critical rotational speed, various wavy modes set in first, then leading to turbulent Taylor Vortex Flow. The onset of TVF, and the transition to WVF strongly depends on the geometry of the system in use. In this study, an important additional factor, namely the surface roughness was investigated using UVP and visual analysis. Radial and axial velocity components were profiled to get information on the vortex shape. Additionally, the onset of TVF and WVF and the frequency of the wavy structure were obtained measuring the radial velocity profile, verifying the visual analysis using Kalliroscope reflective particles. Three different surfaces on the inner rotating cylinder were analyzed for the TVF and WVF regimes. Observing and characterizing the shape of Taylor vortices, a transition point to TVF and WVF was found to be influenced by surface roughness. Namely, the rougher the surface is, the earlier the onset, whereas the onset of WVF is more affected by the geometrical parameter such as the gap size. In addition it can be shown that the surface does not influence the oscillation frequency in the wavy regime but more the gap size. Regarding the shape of vortices, it can be stated out that the ratio between the axial positive velocity ($+V_{z,max}$, upward) and the axial negative velocity ($-V_{z,max}$, downward) is unequal to 1 at the rough wall. In contrast, the ratio at the smooth outer wall is equal to 1 for the whole flow states.

Keywords: Surface Roughness, Taylor-Couette flow, Wavy Vortex flow, Couette cell

1. Introduction

The flow behavior in a rotating coaxial cylinder shows a high periodicity in space and time, and is a well-known platform where flow instability or flow transition to turbulence is investigated. To evaluate the flow state, the Reynolds number or Taylor number is taken into account. Increasing these numbers, shows a sequential transition from Couette flow (CF) to Taylor Vortex Flow (TVF) and Wavy Vortex Flow (WVF) [1]. During such a transition sequence, the flow structure keeps a considerably clear spatial and temporal periodicity. Namely, a roll structure of TVF persists all through and remains even in the highly turbulent regime. WVF shows a clear temporal periodicity arising from an azimuthally wavy structure traveling around the axis. These flow structures were studied since almost 100 years, first by Taylor (1923) [2].

These flow structures offers an efficient continuous cleaning procedure in dynamic membrane filtration. Dispersed particles accumulate on the filter pores and reduce the flux quanti- and qualitatively. The essence of this dynamic filters is a membrane with a rough surface. The influence of the rough surface on the flow structure is rarely analyzed for Taylor Couette cells, more for pipe flow [3-6]. In addition to the roughness of the membrane itself, particles can increase the rough structure when accumulating on the membrane. The formation of TVF in such membrane devices is crucial. It helps to increase the shear on the surface, forcing accumulated particles back into the massflow again.

The aim of this work is to study the influence of the rough surface on the onset and toroid shape of TVF and

WVF. In addition, the oscillation frequency in WVF was analyzed for different rough surfaces in a concentric cylinder device.

2. Experimental

2.1 Fluid system for flow analysis

Glycerol solution (83 wt.%, Thommen-Furler AG) was used to investigate the flow pattern of Newtonian fluids in the flow cell. It has a density of 1,217 g/cm³, with a dynamic viscosity of 65 mPas. Polyamid tracer particles with an averaged size of 90µm and a density of 1,07 g/cm³ (PSP, Met-Flow) were added to the Glycerol solution with a fraction of 1wt.% for UVP measurements and 2wt.%. Kalliroscope particles (Kalliroscope Corporation) were mixed in for visualization of the flow structure.

2.2 Taylor Couette Cell and Surface Roughness measurement

The Couette cell used for the experiments consists of a non-transparent inner PVC cylinder with a radius of $R_I = 59$ mm and a transparent outer Plexiglas cylinder with a radius of $R_O = 70$ mm. Thus, the gap width is $d = 11$ mm and the radius ratio $\eta = R_I/R_O$ is 0,843. The height of the inner cylinder is $L = 250$ mm resulting in an aspect ratio of $\Gamma = d/L = 22,72$. Both ends of the present configuration are attached to the stationary outer cylinder. The inner cylinder was coupled to a motor, which was controlled by a speed inverter (IKA, Staufen, Germany). The gap space between inner and outer cylinder was filled with the fluid system to be measured. The theoretic critical rotational Reynolds number for the onset of TVF is calculated to be

Recrit = 104 [7].

For the simulation of a rough surface, two different sandpapers P80 and P40 (Brütsch & Rüeegg Werkzeuge AG, Switzerland) were used. Therefore, they were glued on the smooth surface cylinder, which increased the inner radius, followed by a reduced gap size. It affects the radius ratio and the critical Reynolds number. The detailed values are summarized up in Table 1.

The difference between smooth and smooth L is the gap width, where the gap of smooth L is adapted to the gap width of P80 and P40. The roughness of P80 corresponds to the roughness of a conventional metal meshed membrane, whereas P40 simulates the membrane with accumulated particles with a size of around 80 μ m.

Table 1: Dimensions of Taylor Couette cell with and without rough surface

	Smooth	Smooth L	P80	P40
Roughness R_a (μ m)	2.1	2.1	45	118
Gap width (mm)	11,0	9,0	9,3	9,0
Radius Ratio (-)	0.84	0.87	0.87	0.87
Critical Reynolds (-)	104	117	116	117

2.3 Instrumentation - UVP

An UVP-Duo instrument (Met-Flow SA, Lausanne, Switzerland) was used to measure the velocity profiles in the flow cell. An ultrasound transducer with 4 MHz basic frequency and 5 mm active and 8 mm housing diameter (Imasonic) was used for axial flow measurements. Profiling of the radial velocity was performed with an 8 MHz transducer with an active diameter of 2.5 mm (8 mm housing). The velocity of sound in the glycerol was measured to be 1794 m/s at 25°C. Further settings are described in Table 2.

Table 2: Setting for the UVP measurements

<i>Axial Velocity Profiling (4MHz)</i>	
PRF	3.56 kHz
Distance between channels	1.12 mm
Cycles per pulse	4
Position of 1. channel	3.14 mm
Amplification (gain)	6-9
<i>Radial Velocity Profiling (8MHz)</i>	
PRF	5.31 kHz
Distance between channels	0.67 mm
Cycles per pulse	4
Position of 1. channel	0.67 mm
Amplification (gain)	6-9

2.4 Procedure

Onset of TVF and WVF and oscillation frequency of WVF – A radial velocity profiling

For onset measurements, the transducer was placed horizontally pointing in the radial direction towards the gap at approximately half of the cylinder height. The frequency of oscillation and radial velocity of the flow in the gap was measured at this position using the UVP with the corresponding setting presented in Table 2. The oscillation frequency could be analyzed with the

corresponding power spectrum. The flow state where a clear peak could be observed was set to be the onset of wavy vortex flow. Similarly, the transition from Taylor flow to azimuthal Couette flow corresponds to the rotational speed of the inner cylinder where Taylor vortices disappear and thus the measured radial velocity component of the flow becomes zero. The UVP data was verified using a visualization technique with Kalliroscope.

Shape of vortices - An axial velocity profiling

The axial velocity profiles in the flow cell were measured with UVP using a 4 MHz - transducer. The transducer was placed in axial position on the bottom close to the inner cylinder and close to the outer cylinder to be able to analyze the whole vortex shape in vertical direction. Therefore, the axial velocity profile could be measured along the inner gap. The resulting output describes the downward (towards the transducer) and upward (away from the transducer) flow. The maximal values of downward and upward flow could be fitted and analyzed.

3. Results and Discussion

3.1 Variation of onset of TVF and WVF

The variation of onset Reynolds number of TVF and WVF is illustrated in Figure 1. The x-axis represents the gap of the concentric cylinder device, where the y-axis shows the onset of TVF (Figure 1a) and WVF (Figure 1b).

Regarding the onset of TVF, it can be stated that it strongly depends on the surface roughness. Both smooth surfaces have an onset of around $Re/Re_{crit} = 0.97$, whereas with increasing roughness the onset is earlier. For P80 it already starts to form vortices at $Re/Re_{crit} =$

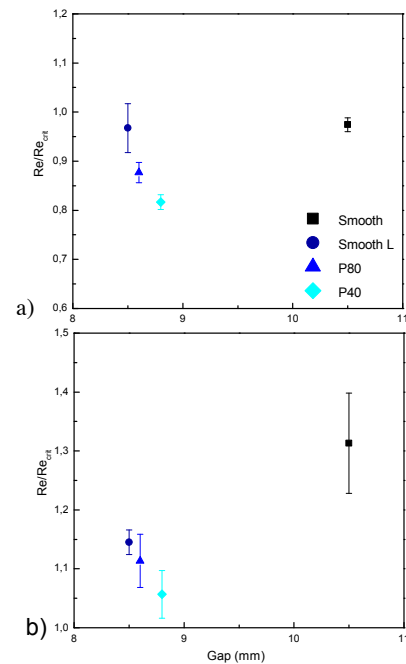


Figure 1: Onset of instabilities with different surface roughness and gap size (a) Onset of TVF is influenced by the surface roughness, whereas, (b) onset of WVF is influenced by the gap size.

0.87 (10% lower) and with P40 it is even more pronounced with an earlier onset of 17% ($Re/Re_{crit} = 0.81$).

In contrast, the onset of WVF is less influenced by the surface roughness, but more on the gap size. Here, smooth L, P80 and P40 have similar gap sizes and onsets of $Re/Re_{crit} = 1.14 / 1.11 / 1.05$. The onset for the smooth surface with a larger gap size is increased to $Re/Re_{crit} = 1.31$.

From these results it can be concluded that the onset of TVF is influenced by a small noise on the surface. The rough surface triggers the flow instabilities and can lead to an overall drag increase [8]. On the other hand, the second instability, WVF, is affected by the spatial characteristics, resulting in a faster onset with increasing gap width.

Another observation is the similar decrease of the onset values for TVF and WVF. The ratio between WVF/TVF-onset is for all cases around 1.3. The energy cascade might explain this phenomenon in flow instability. The increase in Reynolds number means the increase of the energy supply, which is structured in cascade.

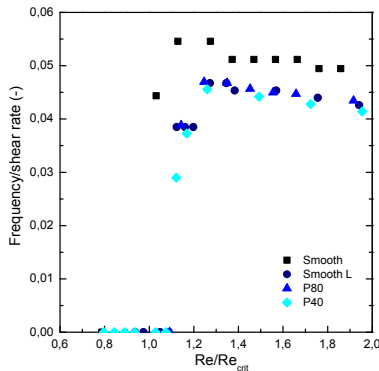


Figure 2: Normalized oscillation frequency of WVF over a range of Re/Re_{crit} for smooth, smooth L, P80 and P40.

3.2 Oscillation frequency of WVF

A detailed observation of the oscillation frequency of wavy flow superimposing the TVF is presented in Figure 2. The azimuthal wavenumber is assumed to be constant for all measurement. The frequency is plotted over the entire range of Re/Re_{crit} and normalized by the shear rate. It gives information on the influence of the rough surface independent on the increase of rotational speed. It can be observed that there is no change in oscillation frequency depending on roughness. It supports the results with the onset of WVF that the gap width more affects the wavy state. The small inner, smooth cylinder has a slightly increased normalized frequency. This leads to an increased travelling speed of the wavy flow, which can be again explained by the spatial characteristics of the wider gap or the change in number of modes.

The decreasing slope could be explained by the non-linear increase of supplied energy to reach a next

energetic mode (modulated wavy). Here a second wave flow is superimposed, which needs energy to be constructed taking it from the wavy state.

3.3 Shape of vortices

In case of smooth cylinder surface, the Taylor vortices adapt the size of the gap and where the ratio of axial upward ($+V_{z,max}$) and axial downward ($-V_{z,max}$) velocity is equal to 1. This is demonstrated in Figure 3, where the round dots represent the smooth cylinder surface. The ratio is the same for the inner and the outer wall of the gap.

Regarding the cylinders with the rough surface, the ratio

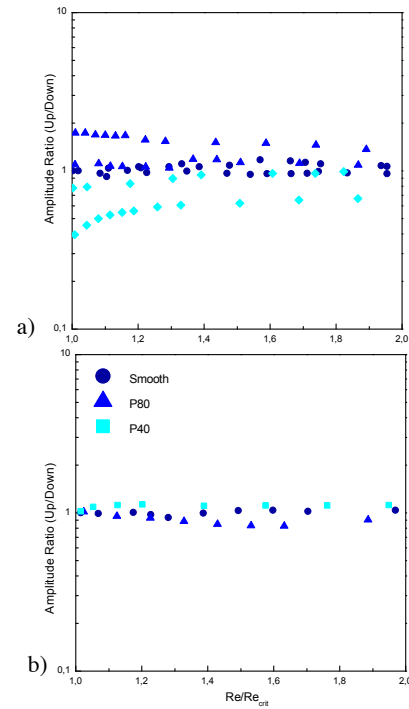


Figure 3: Ratio of $+V_{z,max}$ and $-V_{z,max}$ for different critical Reynolds numbers Re/Re_{crit} for a) inner surface, b) outer surface.

is not equal to 1 for the flow at the inner wall. In case of P80 the upward ($+V_{z,max}$) flow is slightly increased compared to the downward flow at the inner wall. Whereas in case of the rough surface P40 the downward flow is increased at the inner wall, leading to a ratio lower than 1.

A possible explanation is the presence of micro-vortices in the depths of the rough structure. The rotational direction of the inner cylinder forces these vortices into the same direction, which is in this case the downward ($-V_{z,max}$) direction.

4. Conclusion

In this study, the influence of rough surface on flow structure in Taylor Couette cell was analyzed.

It can be concluded that the onset of TVF is strongly influenced by the rough surface. It supports the onset

taking place at lower Reynolds numbers, whereas the onset of WVF is more influenced by the gap width of the system. In addition, it can be stated that the oscillation frequency in WVF regime is not influenced by the roughness but more by the gap width.

Axial velocity measurement showed that the shape of the vortices, namely, the ratio between upward flow and the downward flow is influenced by the rough surface.

These findings have a huge impact on the application fields where dynamic membrane technologies are used and in general, where a rough surface is present in flow. For the calculation of the Reynolds number, the roughness factor has to be considered.

5. Acknowledgements

D. Dufour for introduction into UVP measuring principles; D. Kiechl and B. Pfister for construction of the experimental setup and B. Koller for giving a helpful IT-support.

References

[1] Andereck, C. D., Liu, S. S., Swinney, H. L.: Flow regimes in a circular Couette system with independently rotating cylinders.

Journal of Fluid Mechanics 164 (1986), 155–183.

[2] Taylor, G. I.: Stability of a viscous liquid contained between two rotating cylinders. *Philosophical Transactions of the Royal Society of London A: Mathematical, Physical and Engineering Sciences* 223 (1923), 289–343.

[3] Vijiapurapu, S., Cui, J.: Performance of turbulence models for flows through rough pipes. *Applied Mathematical Modelling* 34 (6) (2010), 1458–1466.

[4] Shockling, M. A., Allen, J. J., Smits, A. J.: Roughness effects in turbulent pipe flow. *Journal of Fluid Mechanics* 564 (2006), 267–285.

[5] Jimnez, J.: Turbulent flows over rough walls. *Annual Review of Fluid Mechanics* 36 (1) (2004), 173–196.

[6] Robertson, J. M., Martin, J. D., Burkhart, T. H.: Turbulent flow in rough pipes. *Industrial & Engineering Chemistry Fundamentals* 7 (2) (1968), 253–265.

[7] Di Prima, R., Swinney, H. L.: Instabilities and transition in flow between concentric rotating cylinders. In: Swinney, H. L., Gollub, J. P. (Eds.), *Hydrodynamic Instabilities and the Transition to Turbulence*. Vol. 45 of *Topics in Applied Physics*. Springer Berlin Heidelberg (1985), 139–180.

[8] van Gils, D. P. M.: Highly turbulent Taylor-Couette flow. Ph.D. thesis, Enschede, 2011.